frontiers | Frontiers in Marine Science

TYPE Original Research
PUBLISHED 14 December 2022
DOI 10.3389/fmars.2022.1094846

OPEN ACCESS

EDITED BY
Wen Zhuang,
Shandong University, China

REVIEWED BY
Xiangbin Ran,
Ministry of Natural Resources, China
Qingzhen Yao,
Ocean University of China, China

*CORRESPONDENCE
Liqin Duan
duanliqin@qdio.ac.cn

SPECIALTY SECTION
This article was submitted to Marine Biogeochemistry, a section of the journal Frontiers in Marine Science

RECEIVED 10 November 2022
ACCEPTED 30 November 2022
PUBLISHED 14 December 2022

CITATION
Fan J, Duan L, Yin M, Yuan H and Li X (2022) Nonconservative behavior of dissolved molybdenum and its potential role in nitrogen cycling in the Bohai and Yellow Seas. *Front. Mar. Sci.* 9:1094846. doi: 10.3389/fmars.2022.1094846

Nonconservative behavior of dissolved molybdenum and its potential role in nitrogen cycling in the Bohai and Yellow Seas

Jinqi Fan[1,2,3,4], Liqin Duan[1,2,3,4]*, Meiling Yin[1,2,3,4], Huamao Yuan[1,2,3,4] and Xuegang Li[1,2,3,4]

[1]CAS Key Laboratory of Marine Ecology and Environmental Sciences, Institute of Oceanology, Chinese Academy of Sciences, Qingdao, China, [2]University of Chinese Academy of Sciences, Beijing, China, [3]Laboratory for Marine Ecology and Environmental Sciences, Qingdao National Laboratory for Marine Science and Technology, Qingdao, China, [4]Center for Ocean Mega-Science, Chinese Academy of Sciences, Qingdao, China

Molybdenum plays an important role in marine biological activity, especially in nitrogen cycling as a cofactor for N_2 fixation and nitrate reductase. However, the dissolved Mo (dMo) behavior and its interaction with N cycling in the coastal waters is still unclear. In this study, the dMo concentrations and parameters related to Mo distribution and N cycling in surface and bottom seawaters of the Bohai (BS) and Yellow Seas (YS) were examined. The results showed that dMo concentrations ranged from 36.4 nmol L^{-1} to 125.0 nmol L^{-1}, most of which deviated significantly from the conservative line, indicating nonconservative behavior of Mo relative to salinity. The highest dMo concentrations occurring in 36°N section of north of the South YS (SYS), were close to conservative value (105 nmol L^{-1}). Significant depletion up to 40-50 nmol L^{-1} of dMo mainly appeared in the BS, NYS and south of the SYS, suggesting the possible removal of dMo by biological utilization and particle adsorption. Particularly, the increasing dMo concentrations away the Yellow River estuary indicated that freshwater dilution was one of reasons for dMo distributions in the BS. The similar spatial distribution of dMo and dissolved Mn concentrations suggested the possible scavenging by MnO_x phases for Mo removal. The negative correlation between dMo and chlorophyll-*a* (Chl-*a*) concentrations in surface seawaters suggested that biological uptake was involved in dMo removal. The depleted dMo in most of sites corresponded with the higher nitrite concentrations, implying the possible involvement of nitrate reduction process. Although the highest N_2 fixation rates and relative abundances of cyanobacteria appeared in 36°N section, corresponding with the conservative dMo, suggesting that Mo may play a minor role in N_2 fixation process there. The ten-folds of relative abundance of bacteria with nitrate reduction function than that with N_2 fixation function suggested that dMo seems to play more important role in nitration reduction than nitrogen fixation in the BS and YS.

KEYWORDS

dissolved molybdenum, nonconservative behavior, biological uptake, N_2 fixation, nitrate reduction

1 Introduction

As the most abundant transition metal, molybdenum (Mo) exists mainly as in the dissolved forms (MoO_4^{2-}, $HMoO_4^-$) in the oxygenated ocean. Dissolved Mo (dMo) concentrations are stable in the open ocean, with reported concentrations between 105 and 107 nmol L^{-1} (Collier, 1985; Smedley and Kinniburgh, 2017). DMo shows a conservative characteristic in the open ocean (Audry et al., 2007; Beck et al., 2012; Valdivieso-Ojeda et al., 2020). The constant stable isotope ratio of Mo in the ocean also suggests the relative unreactivity of oceanic Mo (Nakagawa et al., 2012; Ho et al., 2018). However, dMo in several estuaries and coastal areas showed non-conservative behavior (Dellwig et al., 2007; Wang et al., 2016; Ho et al., 2018). Various dMo concentrations in different costal and estuarine waters were found, with most of dMo depleted. For example, dMo in Mississippi Estuary (Mohajerin et al., 2016), Itchen Estuary (Archer and Vance, 2008), multiple estuaries in India (Rahaman et al., 2010), Wadden Sea (Dellwig et al., 2007), and Taiwan Strait (Wang et al., 2016) displayed depletion and nonconservative behavior. The reasons for Mo depletion are varied and likely related to biological processes, scavenging by particles (e.g., Fe/Mn oxides), and sedimentary interactions (Reitz et al., 2007; Ho et al., 2018). The Mo excess in some studies is attributed to extra sources, e.g., porewater diffusion at sediment-water interface (Dellwig et al., 2007; Strady et al., 2009; Waeles et al., 2013), submarine groundwater discharge (Dalai et al., 2005), and industrial discharge (Rahaman et al., 2010; Wang et al., 2016).

The main abiotic processes affecting dMo distribution in the coastal waters are riverine input and particle adsorption. Molybdenum entering into the oceans mainly by riverine input after oxidative weathering on the land (Zerkle et al., 2011). Rivers have supplied ~22,000 t a^{-1} of Mo to the oceans (Smedley and Kinniburgh, 2017), accounting to~90% of total dMo (Morford and Emerson, 1999; Wang et al., 2016). Riverine Mo concentrations are low, with the estimated values of ~4.38 nmol L^{-1} (Chen et al., 2014) and 1.15-89.9 nmol L^{-1} (Linnik et al., 2015) in the world rivers. Thus, dMo generally displays an increase with the increasing salinity of estuaries due to the freshwater dilution. A non-biotic adsorption onto MnO_x phases has been proved one reason for Mo depletion (Dellwig et al., 2007). It has been found that dMo had a positive correlation with dissolved Mn (Wang et al., 2016) and a negative correlation with particle Mn (Dellwig et al., 2007), suggesting the scavenging of dMo by MnO_x phase. The scavenging and deposition of dMo with ferromanganese oxides accounts for ~35% of removal of modern marine Mo (Scott et al., 2008; Zerkle et al., 2011).

Molybdenum is an essential element for N_2 and nitrate assimilation due to it is a cofactor for some N_2 fixation and nitrate reductase (Wolfe, 1954; Fay and Fogg, 1962; Robson et al., 1986; Fischer et al., 2005). Thus, Mo depletion is more related to biotic processes. Extremely low dMo concentration (<3 nmol L^{-1}) can limit heterotroph growth in freshwater and seawater (Glass et al., 2012; Wang et al., 2016). Mo scarcity (0.6-4 nmol L^{-1}) in some lakes also can limit phytoplankton growth (Goldman, 1960; Glass et al., 2010; Glass et al., 2012). However, the influence of biological uptake on Mo removal in the coastal waters is still unclear. The higher cellular Mo concentrations in phytoplankton (~5.3 μmol L^{-1}; Ho et al., 2003) and bacteria (53 μmol L^{-1}; Barton et al., 2007) than in seawater suggest that marine algae and heterotrophs could consume dMo and contribute to the dMo depletion in water column (Wang et al., 2016). The negative correlation between Chl-*a* and dMo were observed in both the coastal waters (Wang et al., 2016) and open sea (Ho et al., 2018), further suggesting the involvement of biological uptake in removing dMo out of the water column.

The Mo removal by utilization of nitrogen fixation organisms were observed in cultures. For example, the addition of Mo and NO_3^- in the hypolimnion of Castle Lake could promote nitrogen assimilation protein activity increase when NH_4^+ was scarce (Glass et al., 2012). However, the limitation of Mo on nitrogen fixation in the ocean has not been found or not been studied. Positive and negative Mo concentration anomalies were found in N_2 fixation in the Eastern Equatorial Pacific (+5 nmol L^{-1}, -3 nmol L^{-1}; Tuit and Ravizza, 2003), presumably related to biological nitrogen fixation processes (Dellwig et al., 2007). In addition, the Mo removal also is related to the utilization by marine algae and/or cyanobacteria with nitrate reductase. Ho et al. (2018) has found that some depleted dMo corresponded with the nitrite maximum in the oxygen deficient zone (ODZ) off the Peru margin, suggesting that Mo likely involved in nitrate reduction.

Marine nitrogen fixation and denitrification are two important processes in the nitrogen cycle, which play a key role in understanding marine nitrogen fixation, nitrogen loss and nitrogen budget balance (Fowler et al., 2013). In particular, the recent studies have found that the marginal seas may be a potential hotspot for nitrogen fixing organisms (Zehr and Capone, 2020; Qu et al., 2022). However, the dMo behavior and its interaction with N cycling in the coastal waters is still unclear. The Bohai Sea (BS) and Yellow Sea (YS) are one of main marginal seas in China, receiving a large amount of inorganic nutrients from terrestrial sources. The DIN concentration in the BS and YS underwent a 6-7-fold increase from the late 1990s to the 2010s (Xin et al., 2019; Zheng and Zhai, 2021), inducing a DIN/DIP ratio increase and DSi/DIN ratio decline (Liu et al., 2011; Guo et al., 2014). Their biological activities also are frequent. In this study, dMo concentrations and parameters related to Mo distribution and N cycling in surface and bottom seawaters of the BS and YS were examined. The aim is to identify dMo behavior and its potential regulatory role in nitrogen cycling of the BS and YS.

2 Materials and methods

2.1 Study area

The BS and YS are typical semi-enclosed continental shelf seas, located in the western Pacific Ocean between mainland China and the Korean Peninsula. The BS has the area of 77×10^3 km^2 and average depth of 18 m with the maximum depth of 83 m in the Bohai Strait. The YS has the area of 380×10^3 km^2 and average depth of 44 m with a maximum depth of 140 m. The Yellow River (YR) is the main river entering the BS, with the freshwater influx of ~200×10^8 m^3 a^{-1} (Xu et al., 2013). The main current in the BS is the Bohai Sea Coastal Current (BSCC), which can carry low-temperature, low-salinity and high nutrients into the YS under the influence of northwest monsoon (Chen, 2009). However, the currents in the YS are complex. The interaction among monsoon, bottom topography, river discharge and the Kuroshio intrusion leads to various circulation regimes and different water masses. The seasonal circulation is mainly reflected in the Yellow Sea Warm Current (YSWW). In summer and autumn, the YSWW moves northward under the influence of southeast monsoon. In winter, the YSWW forms a circulation in the SYS region affected by northeast monsoon (Chen, 2009). This study focused on autumn, when there are the Yellow Sea Coastal Current (YSCC) in the west, the South Korean Coastal Current (WKCC) in the east, and the YSWW in the middle of the SYS, which can move northward through the Bohai Strait into the BS. In addition, there is a typical seasonal cold water mass in the YS, namely the Yellow Sea Cold Water (YSCW). The YSCW (<12°C) mainly appears in summer and autumn when the southwest monsoon prevails. The YSCW exhibits low temperature and high salinity characteristics (Wang et al., 2014). In addition, the low DO and pH values also are found in the YSCW (Zhai, 2018; Guo et al., 2020).

The sample collection in the BS and YS was conducted aboard the R/V *Lan Hai 101* in 18 October and 4 November 2021 (Figure 1). Seawater samples at surface (2 m) and bottom (2 m above seafloor) layers were collected at 38 stations using 12-L Niskin bottles for dMo, nutrients, chlorophyll-*a* (Chl-*a*), dissolved oxygen (DO) and pH. The water sampler was installed on a rosette with a Seabird conductivity, temperature, depth (CTD) sensor to determine *in situ* temperature, salinity and depth. Seawater samples for DO and pH measurement were collected firstly. Seawater samples for dMo and nutrients were filtered through 0.45 μm Nuclepore® polycarbonate membrane filters previously cleaned with 5% HCl. Samples were filtered into pre-cleaned HDPE bottles and immediately acidified with ultrapure HCl to pH<2. Another part of filtered seawaters was collected in acid-clean, 60 ml HDPE bottles and stored at -20°C for nutrient analysis. Samples for Chl-*a* were filtered through cellulose acetate fiber filters (0.45μm pore size; Whatman) and

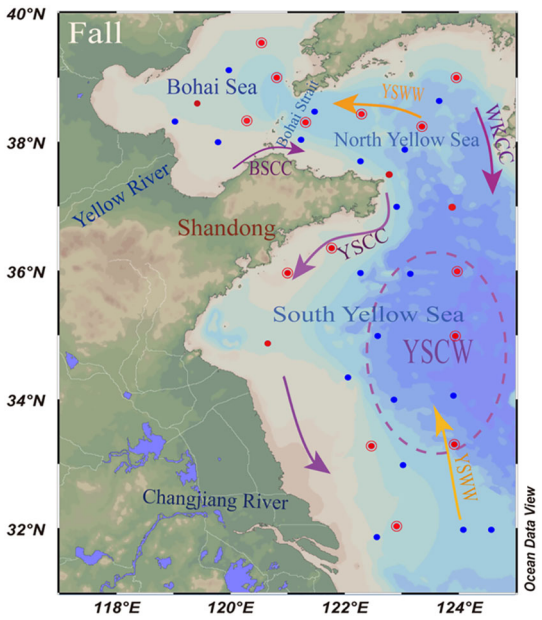

FIGURE 1
Study area and sampling sites in the Bohai Sea (BS) and Yellow Sea (YS) between 18 October and 4 November 2021. Temperature, salinity, DO, inorganic nutrients, Chl-*a* and dMo concentrations in surface and bottom seawater at all stations (blue + red) were determined. N_2-fixation rates at 14 stations (red hollow circles) and 16s rRNA at 18 stations (red solid dots) were measured in surface seawaters. In autumn, the circulation schematic includes the Bohai Sea Coastal Current (BSCC), Yellow Sea Coastal Current (YSCC), Western Korean Coastal Current (WKCC) and Yellow Sea Warm Water mass (YSWW). The Yellow Sea cold water (YSCW) is located in the dashed circles.

stored in dark at -20°C until further analysis in the laboratory. Microbial samples at 18 stations were collected by filtering 1 L of seawater through a 0.2 μm polycarbonate membrane. After filtration, the samples were kept in cryovials and stored at -80°C.

Surface seawaters at 14 stations were collected for nitrogen fixation incubations. 1 L surface seawater was collected and filtered immediately before the incubation period for determining the particulate ^{15}N abundance in original seawater. The N_2 fixation rates (NFRs) were determined using the $^{15}N_2$ gas dissolution method described in Mohr et al. (2010). The $^{15}N_2$-enrich seawater was prepared using $^{15}N_2$ gas at each station. Briefly, the filtered seawater was degassed and 1 ml of 99 atom% pure $^{15}N_2$ gas was injected into 100 ml of degassed seawater using the method described by Mohr et al. (2010). Unfiltered Seawater was added to duplicate acid-cleaned 600 ml polycarbonate bottles slowly to avoid air bubbles. Before incubation, 45 ml of seawater was removed from bottle. Then, 45 ml of $^{15}N_2$-enrich seawater was injected into incubation bottles. Each incubation bottle was shaken 5 times to ensure that water was fully mixed. Incubation was performed in incubator with continuous *in situ* seawater flow under natural

light for 24 h. After incubation, seawater was filtered (<100 mm Hg) *via* pre-combusted (450°C, 5 h) Whatman GF/F filter and stored at -20°C for determining the particulate ^{15}N abundance.

2.3 Sample analysis

2.3.1 DO and pH

The DO concentration and pH were determined using a Seven Excellence Multiparameter (Mettler Toledo, US) equipped with the DO and pH probes. The DO values were calibrated by the Winkler titration method (Bryan et al., 1976). The pH was calibrated to the *in situ* value by seawater temperature.

2.3.2 Dissolved Mo and Mn

Dissolved Mo and Mn concentrations were determined by inductively coupled plasma mass spectrometry (ICP-MS, Thermo iCAP Q) after 10-fold dilution with 0.4 M ultrapure HNO_3. Helium and KED were used as collision gas and mode of interference elimination. Internal standards Y for Mo and Sc for Mn were chosen. Certified reference material NASS-6 was used to ensure accuracy of the analytical procedure with accuracy of 98.0% for Mo and 96.2% for Mn. Replicate measurement was conducted on NASS-6 and samples with the relative standard deviations (RSD) of 4.5% for Mo and 7.6% for Mn. Procedural acid blanks for diluting samples were determined every 10 samples. The acid blanks are lower than the detection limits.

2.3.3 Nutrients and Chl-*a*

Nutrients including nitrate (NO_3-N), nitrite (NO_2-N), ammonium (NH_4-N), phosphate (PO_4-P) and silicate (SiO_3-Si) were determined photometrically using a continuous segmented flow analyzer (QuAAtro, Bran-Luebbe Inc., Germany). Their detection limits were 0.02 μmol L^{-1}, 0.02 μmol L^{-1}, 0.03 μmol L^{-1}, 0.01 μmol L^{-1} and 0.04 μmol L^{-1}, respectively. The standard deviation (SD) of three measurements was< 3%. Dissolved inorganic nitrogen (DIN) includes NO_3-N, NO_2-N and NH_4-N.

The filters for Chl-*a* were extracted with N, N-dimethylformamide for 12 h at 4°C. The extracts were measured using a fluorescence spectrophotometer (F-4500, Hitachi Co, Japan). Its detection limit was 1.5 μg L^{-1} with SD of<1% for 11 parallel determinations.

2.3.4 Bacteria abundance

The DNA was extracted by QIAquick Gel Extraction Kit (Qiagen, Germany). The PCR amplifications were conducted with the 515f/806r primer set that amplifies the V4 region of the 16S rRNA gene. High-throughput sequencing was carried out on the Illumina HiSeq 2500 platform (Illumana, San Diego, USA) by Novogene Technology Co., Ltd. (Beijing, China). The sequences with 96% similarity were classified into the identical operational taxonomic units (OTUs). Taxonomic data were assigned by Ribosomal Database Project (RDP) classifiers. The relative abundance of cyanobacteria at the phylum-level was used in this study.

2.3.5 N_2 fixation rate

Filters were freeze-dried and then determined by an Elemental Analyzer (Thermo Flash 2000)-Isotope Ratio Mass Spectrometer (Thermo-MAT253) to determine the natural and tracer-enriched ^{15}N abundances. The calculation formula of NFR is as follows (Mohr et al., 2010):

$$NFR = \frac{(A_{PN}^{final} - A_{PN}^{t=0})}{(A_{N_2} - A_{PN}^{t=0})} \times \frac{1}{\Delta t}\left(\frac{PN_f + PN_0}{2}\right)$$

where A = atom% ^{15}N in the particulate organic nitrogen (PN) or dissolved N_2 at the final or beginning (t = 0) of incubation, Δt is the incubation time (d), A_{N2} represents the nitrogen substrate in the system at the beginning of the culture. The formula is as follows:

$$A_{N_2}(\%) = \left(\frac{A_S \times V_S + A_{atm} \times C \times V_b}{V_s + C \times V_b}\right) \times 100$$

where A_{atm} and A_S are the atomic percentages of ^{15}N in atmospheric N_2 (0.366%) and in the added ^{15}N tracer (98%), V_b and V_S are the volumes of the culture system (L) and the ^{15}N tracer (mL), C is the N_2 concentration in the culture water.

2.4 Statistical analysis

Pearson correlation analysis using SPSS 16.0 was used to determine the relationships among the dMo, dMn, Chl-*a*, nutrients, NFR, relative abundance of cyanobacterial, N_2 fixation functional bacteria and nitrate reduction functional bacteria in the BS and YS. P< 0.05 (two-tailed) values were considered significant correlations. Origin 2021 and Ocean Date View 2021 ware used to plot the data.

3 Results

3.1 Dissolved Mo and Mn

The dMo had similar concentration ranges between surface (76.4 ± 19.2 nmol L^{-1}) and bottom (74.6 ± 22.4 nmol L^{-1}) seawaters in the BS and YS. The lowest dMo values (68.9 ± 17.0 nmol L^{-1} in surface and 64.5 ± 19.1 nmol L^{-1} in bottom) were in the BS, while the highest dMo concentrations (95.9 ± 21.0 nmol L^{-1} in surface, and 94.9 ± 19.2 nmol L^{-1} in bottom) appeared in north of the SYS (near 36°N; Figure 2A). In the YSCW, the dMo concentrations in surface seawaters were slightly higher than that in bottom ones, but it showed the opposite trend in the other areas (Table S1).

The dissolved Mn (dMn) concentrations in surface seawaters (1.06 ± 1.87 μmol L^{-1}) were higher than that in bottom seawaters (0.52 ± 0.89 μmol L^{-1}; Figure 2B). In surface seawaters, the highest dMn values appeared at surface above the YSCW (2.45 ± 2.32 μmol L^{-1}) and station (1.50 ± 2.36 μmol L^{-1}) in 36°N section, followed by the nearshore station. In bottom seawaters, the higher dMn values occurred at nearshore of the SYS.

3.2 Hydrochemical characteristics

The temperature in surface seawaters (19.1 ± 2.1°C) was higher than that in bottom seawaters (16.7 ± 4.1°C) in the BS and YS in autumn. However, the temperature in bottom seawaters showed abnormally low values (10.4 ± 1.0°C) in the YSCW (Figure 3A). The salinity in surface seawaters (30.62 ± 1.65) was lower than that in bottom seawaters (31.16 ± 0.90) in the BS and YS. There were abnormally high salinity values (32.37 ± 0.41) in bottom seawaters of the YSCW (Figure 3B). The pH in surface seawaters (8.12 ± 0.11) was higher than that in bottom seawaters (8.05 ± 0.06) in the BS and YS. The relatively high pH in surface seawaters appeared at nearshore and above the YSCW (Figure 3C). The DO concentrations in surface seawaters (7.5 ± 0. 7 mg L^{-1}) was higher than that in bottom seawaters (7.0 ± 0.6 mg L^{-1}) in the BS and YS (Figure 3D). There were abnormally low pH (8.07 ± 0.05) and DO values (6.3 ± 0.3 mg L^{-1}) in bottom seawaters of the YSCW. The Chl-*a* concentrations in surface seawaters (2.10 ± 4.00 μg L^{-1}) was higher than that in bottom seawaters (0.98 ± 0.86 μg L^{-1}) in the BS and YS. The Chl-*a* concentrations decreased from the BS to the NYS and to the SYS and from nearshore to the outer seas (Figure 3E; Table S2).

3.3 Inorganic nutrients

The nutrient concentrations in surface and bottom seawaters of the BS and YS were examined (Figure 4). Concentrations of DIN, PO_4-P and SiO_3-Si in surface seawaters (DIN: 3.12-23.0 μmol L^{-1}; PO_4-P: 0.08-0.61 μmol L^{-1}; SiO_3-Si: 1.29-12.7 μmol L^{-1}) were lower than that in bottom seawaters (DIN: 3.15-24.8 μmol L^{-1}; PO_4-P: 0.04-1.81 μmol L^{-1}; SiO_3-Si: 1.12-15.6 μmol L^{-1}) in the BS and YS in autumn (Table S1). NH_4-N and NO_3-N were the main forms of DIN, accounting for 55% and 41%. PO_4-P, DIN and SiO_3-Si concentrations generally presented the highest values in the BS, followed by the NYS and the SYS. Besides, they also displayed higher values in the YSCW. Outside the YSCW region, nutrients displayed negative correlations with salinity in the SYS, but only PO_4-P presented a relatively conservative behavior ($r=-0.546$, $p<0.01$).

3.4 N_2 fixation rates and cyanobacteria abundances

The NFRs and relative abundances of cyanobacteria in surface seawaters of the BS and YS were determined. The NFRs were 0.11-1.05 nmol N L^{-1} d^{-1}. The highest NFRs were in the SYS (0.55 ± 0.27 nmol N L^{-1} d^{-1}), followed by the NYS (0.42 ± 0.09 nmol N L^{-1} d^{-1}) and the BS (0.13 ± 0.17 nmol N L^{-1} d^{-1}; Figure 5A). The highest NFR appeared in north of the SYS (near 36°N). Similarly, the highest relative abundances of cyanobacteria were in the SYS (27.0 ± 19.3%), followed by the NYS (18.7 ± 10.1%) and BS (7.0 ± 10.2%), with the highest values in north of the SYS (near 36°N; Figure 5B).

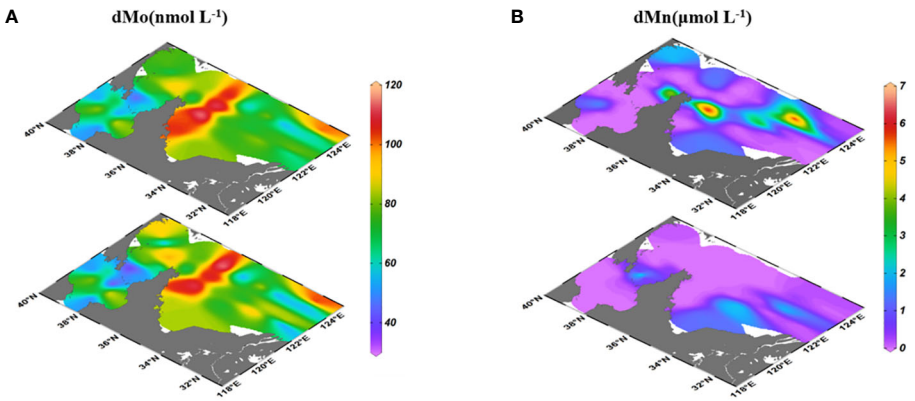

FIGURE 2
Distributions of dMo **(A)** and dMn **(B)** in surface and bottom seawaters of the BS and YS.

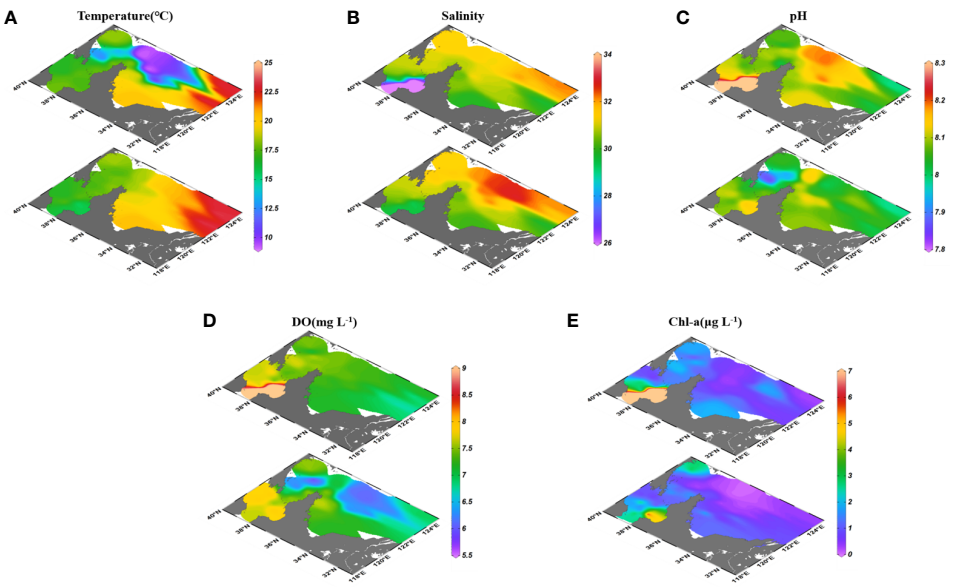

FIGURE 3
Distributions of hydrochemical parameters temperature **(A)**, salinity **(B)**, pH **(C)**, DO **(D)** and Chl-*a* **(E)** in surface and bottom seawaters of the BS and YS.

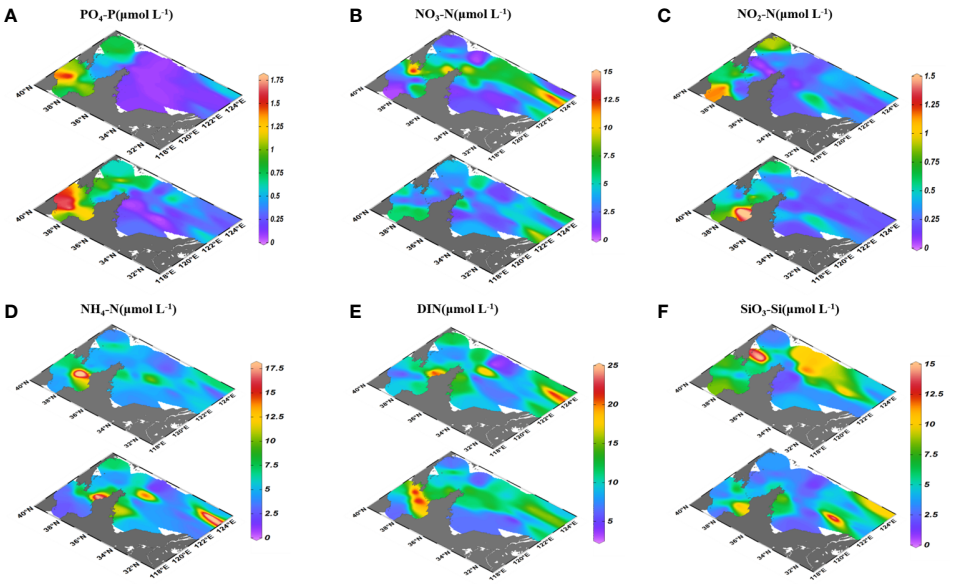

FIGURE 4
Distributions of PO_4-P **(A)**, NO_3-N **(B)**, NO_2-N **(C)**, NH_4-N **(D)**, DIN **(E)** and SiO_3-Si **(F)** in surface and bottom seawaters of the BS and YS.

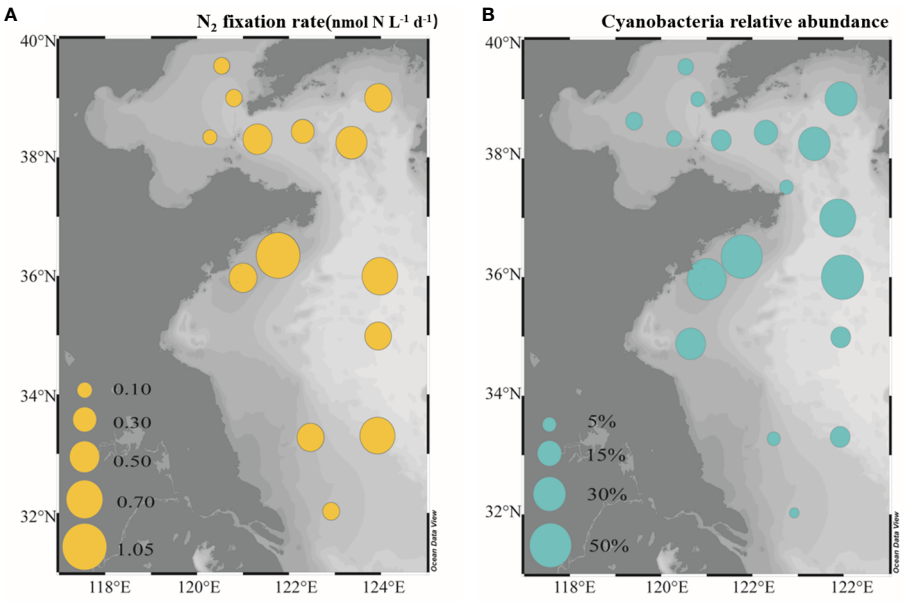

FIGURE 5
Distribution of N_2 fixation rates **(A)** and the relative abundance of cyanobacteria **(B)** in surface seawaters of the BS and YS.

4 Discussion

4.1 Nonconservative behavior of dMo

Despite its biological requirement, Mo generally shows a conservative behavior independent of marine biological activities (Collier, 1985; Prange and Kremling, 1985). The conservative behavior of dMo in some estuaries also were found (Strady et al., 2009; Waeles et al., 2013). In these estuaries, dMo concentrations showed a closely liner relationship with salinity due to the dilution of Mo-rich seawaters by river waters with lower biological activity (Howarth and Cole, 1985; Strady et al., 2009). Differently, dMo concentrations in our study area had no correlation with salinity (Figure 6), indicating that conservative mixing with river waters was not the dominating process and thus the nonconservative property of dMo in the BS and YS. Most of dMo concentrations in the BS and YS were below a conservative mixing and were depleted by more than ~30%. Significant depletion up to 40-50 nmol L^{-1} of dMo was even seen in the BS and NYS regions. The dMo removal was attributed to scavenging by abiogenic and/or biogenic particles in the mixing process (Prange and Kremling, 1985). The lowest dMo concentration (49.1 nmol L^{-1}) occurred in station (S=23.6) near the Yellow River in the BS, which was lower than its concentration in conservative estuaries with the same salinity (Rahaman et al., 2010; Waeles et al., 2013). This seems to suggest that although the riverine input played an important role in dMo distribution there, there still was other reasons for dMo depletion. For example, the biological uptake and complexation with organic matter or incorporation into sediment aggregates could contribute to the dMo removal (Head and Burton, 1970; Dellwig et al., 2007).

In contrary, some dMo concentrations in the BS and YS were higher than those expected for a conservative mixing. The

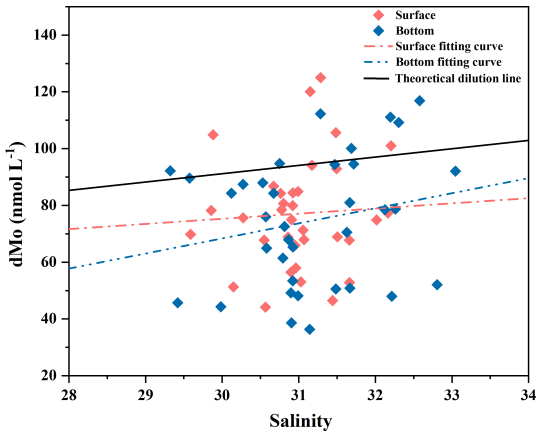

FIGURE 6
The plot of dMo against salinity in the BS and YS. Blue and red dots respect values in surface and bottom seawaters, respectively. The black line represents the theoretical mixing line between river water (dMo = 1 nmol L^{-1}) and ocean water (dMo = 105 nmol L^{-1}) at salinity of 35.

addition of dMo mainly appeared at 36 °N section and bottom seawaters in south of the SYS. It has been suggested that the addition of Mo resulted from its desorption from particles or release from bottom sediments when bottom redox condition changed from reducing to oxic (Dalai et al., 2005; Morford et al., 2007; Smedley and Kinniburgh, 2017). Due to the significant differences in the hydrochemistry and biological activities among the BS, NYS and SYS, the main control factors of nonconservative Mo behavior in these three sea areas were different. This will be discussed in the below section.

Compared with horizontal distribution, vertical difference of dMo concentrations was small, suggesting the influencing factors at different depth of same station was more similar than regional differences due to the relatively shallow depths of the study area. Compared with other sea areas in the world (Table 1), dMo concentrations in the BS and YS (36.4-125.0 nmo L^{-1}) were similar to the nonconservative dMo in other estuaries (Khan and Van Den Berg, 1989; Dalai et al., 2005; Dellwig et al., 2007; Archer and Vance, 2008; Rahaman et al., 2010; Mohajerin et al., 2016; Schneider et al., 2016; Smedley and Kinniburgh, 2017), but lower than the open ocean (Firdaus et al., 2008; Ho et al., 2018) and higher than the euxinic seas (Neal and Robson, 2000; Rahaman et al., 2010; Chen et al., 2014).

4.2 The physics and chemistry processes involved into Mo cycling

4.2.1 The riverine dilution and particle adsorption of dMo

The increase of dMo from the coast toward offshore was mainly observed in the BS, especially off the Yellow River estuary. The area off the estuary was characterized by low dMo concentrations mainly due to the river discharge from the Yellow River with low Mo concentration. Previous study had also attributed the occurrence of dMo depletion in estuary to the dilution effect of freshwater (Waeles et al., 2013). Although we did not determine dMo concentrations in the Yellow River, it has been suggested that average dMo concentration in world rivers was ~12.6 nmol L^{-1} (Linnik et al., 2015). Besides, in autumn, under the influence of the northwest monsoon, a large amount of the BS water flows into the NYS through the Bohai Strait (Zhang et al., 2018), resulting in the lower dMo in the Bohai Strait.

The horizontal and vertical differences of dMo could not be attributed solely to the freshwater dilution effect. The importance of Mn cycling to Mo behavior has been found. It has been suggested that the removal of MoO_4^{2-} from surface seawaters was associated with Mn oxidation and adsorption by freshly formed MnO_x phases, which would settle on the sediments (Dellwig et al., 2007). In this study, both dMo and dMn presented the highest values in the SYS, followed by the NYS, and the lowest in the BS. This distribution was opposite to DO concentrations, likely suggesting that high DO level might favor the formation of Mn oxides and associated Mo adsorption. There was a significant positive correlation ($r=0.55$, $p<0.01$; Figure 7A) between dMo and dMn in the BS and YS except for the area with extremely high dMn values. The more significant correlation was found in the BS ($r=0.89$, $p<0.01$; Figure 7B), suggesting that the role of the adsorption to inorganic particles to remove dMo in the BS was more important than in the YS.

4.2.2 Effect of seasonal YSCW on dMo

The YSCW is an important current, supplying abundant nutrients to upper seawaters and stimulating the algal blooms (Guo et al., 2020). Thus, it is necessary to discuss the influence of the YSCW on dMo depletion. The dMo concentrations in both surface and bottom seawaters displayed low values in the YSCW. However, the slightly higher dMn values in surface seawaters than bottom seawaters, indicating that the adsorption by inorganic particles with MnO_x may be not the main reason for Mo depletion there.

The YSCW is a seasonal current, which usually appears in summer and autumn. It has low DO, low temperature and high salinity (Wang et al., 2014). The same phenomenon was observed in this study (Figure 8). Mo as a redox-sensitive element, seasonal DO change has an important influence on the dynamics of dMo. Particularly, the relatively low DO in the YSCW contributed to the Mo removal from bottom seawaters to sediments. Morford et al. (2007) has found that Mo could be sequestered into sediments along

TABLE 1 Dissolved molybdenum concentrations in estuaries and open seas in the world.

Sea area	dMo (nmo L^{-1})	References
Tamar Estuary, England	15.0-89.9	(Khan and Van Den Berg, 1989)
Chao Phraya Estuary, Thailand	3.20-117	(Dalai et al., 2005)
Estuary of Wadden Sea, Germany	82.3-156	(Dellwig et al., 2007)
Itchen Estuary, England	4.79-117	(Archer and Vance, 2008)
Multiple estuaries, India	1.00-89.6	(Rahaman et al., 2010)
Mississippi Estuary, United States	9.10-55.9	(Mohajerin et al., 2016)
Elbe, Rhine and Weser estuaries	20.0-125	(Schneider et al., 2016)
Oxic open water,	96.9-108	(Firdaus et al., 2008; Ho et al., 2018)
Euxinic Black Sea	7.00-39.0	(Neal and Robson, 2000;Nagler et al., 2011)

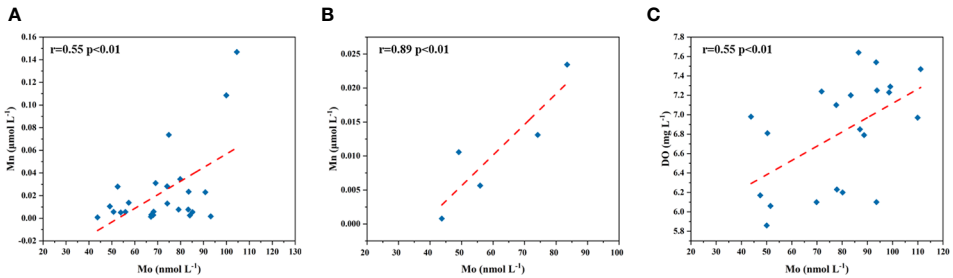

FIGURE 7
Correlations between dMo and dMn concentrations in surface seawaters of the BS and YS **(A)** and that of the BS **(B)**, and correlation between DO and dMo concentrations in bottom seawaters of the YS **(C)**.

the western Indian continental shelf when seasonal oxygen minimum zone appeared. However, sedimentary Mo can be later released to bottom seawater when oxic condition appeared. The strong upwelling in this region can carry bottom Mo to the surface (Smedley and Kinniburgh, 2017). Sulu-Gambari et al. (2017) found a clear Mo enrichment in the upper sediment layer in anoxic summer and autumn, whereas small Mo enrichment in oxic winter and spring. Our results showed that the lower bottom dMo concentrations in the YSCW was consistent with the lower DO concentrations, suggesting that dMo in bottom seawaters moved into sediments or the release of dMo from porewater was restricted under low DO levels in autumn. Within sediments, MoO_4^{2-} can be fixed by thiol and buried as sulfide in high sulfide sedimentary environment, resulting in Mo enrichments in marine sediments (Brumsack, 2006). The upward transport of dMo was also prevented due to the water stratification in the YSCW. This part of oxidative Mo (MoO_4^{2-}) may be released into seawaters *via* the sediment/water interface when the YSCW disappeared in winter and spring. This speculation requires further confirmation. There was a significant correlation between DO and dMo concentrations in bottom seawaters of the YS (except for stations near 36°N and the Bohai Strait) (r=0.55, p<0.01; Figure 7C), further suggesting that the higher DO level favored the dMo release from sediment while lower DO attenuated this process.

4.3 The biological processes involved into Mo cycling

4.3.1 Phytoplankton utilization of dMo

Mo exists in >60 enzyme cofactors (Stiefel, 1996) and involved in catalyzing key processes in the global carbon, sulfur and nitrogen cycles (Mendel, 2009). Both phytoplankton

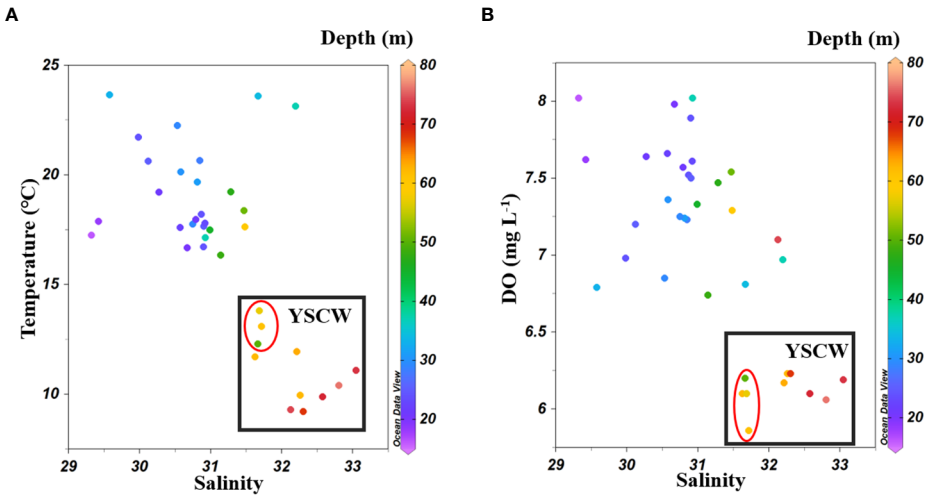

FIGURE 8
Scatter plots of bottom sea water salinity and temperature **(A)**, and salinity and DO **(B)** in the BS and YS. The Yellow Sea Cold Water (YSCW) was boxed in black rectangle and stations in the NYS affected by YSCW circled in red oval.

and heterotrophs require Mo participating in metabolic activities (Glass et al., 2012). It has been found that the Mo concentrations in phytoplankton (Ho et al., 2003) and bacterial (Barton et al., 2007) cells were far higher than in seawater, suggesting that the high abundances of phytoplankton and bacteria may consume a large amount of dMo, and may cause the dMo removal in seawater (Wang et al., 2016). Especially, the more depleted dMo can occur in phytoplankton blooms (Kowalski et al., 2009). Our results showed that more depleted dMo concentrations appeared in the BS and the NYS, where Chl-*a* concentrations were higher. The negative correlation of dMo with Chl-*a* (except for two extremely high Chl-*a* in the BS) (r= -0.45, p<0.01; Figure 9A) in the BS and YS indicated that high primary productivity likely played an important role in the dMo removal. Their correlations were most significant in the BS (r= -0.97, p<0.01; Figure 9B), followed by the NYS (r=-0.60, p<0.01; Figure 9C) and the SYS (r= -0.42, p<0.01; Figure 9D), suggesting that the uptake of phytoplankton was more important removal mechanism for dMo in the BS than the YS. The dMo removal by phytoplankton utilization also has been found in other sea areas, such as the Southampton estuary (Head and Burton, 1970), the Taiwan Strait (Wang et al., 2016), and East Pacific Zonal Transect (Ho et al., 2018). However, Chl-*a* and nutrients (especially PO_4-P and SiO_3-Si) might have the obvious low values in 36 °N section, corresponding to the conservative dMo concentrations, suggesting that low biological activity had little effect on the Mo removal there.

According to the estimation method of Wang et al. (2016), Chl-*a* level of 5 μmol L^{-1} as 5 × 10^6 cells mL^{-1} and cellular Mo of 5.3 μmol L^{-1} in phytoplankton (Ho et al., 2003) were used to estimate the depletion of dMo by phytoplankton. The whole BS and YS was assumed to be an enclosed system in autumn, and Chl-*a* values in the BS and YS and were used. The depletion of dMo and biological removal amount of Mo were estimated to be up to 50 nmol L^{-1} with an average of 20 nmol L^{-1} and 8.9×10^7 mol if a bloom continued for 1 month. The biological removal amount was obtained by multiplying the depleted Mo concentration with the water volume (457×10^{10} m^3) in the upper layer of the BS and YS (from surface to 10 m).

4.3.2 Coupling of dMo to nitrogen cycling

Mo is key for microbial N_2 and nitrate assimilation due to its presence in nitrogenase and nitrate reductase (the first step in NO_3^- assimilation). Marine and freshwater diazotrophic cyanobacteria

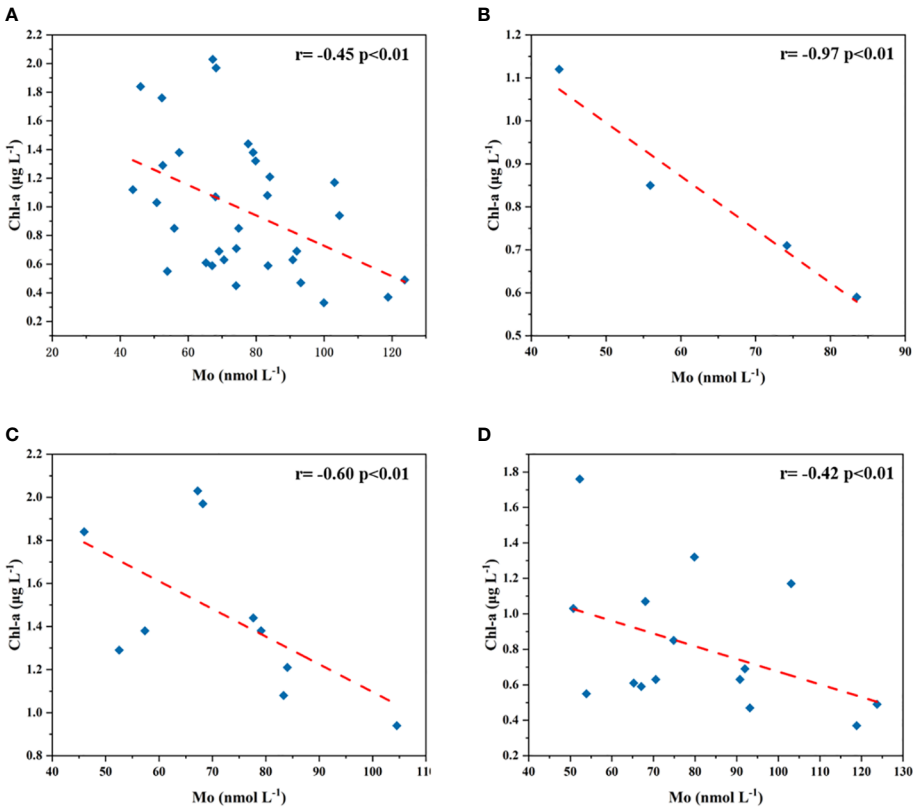

FIGURE 9
Correlations of dMo with Chl-*a* in the BS and YS **(A)**, the BS **(B)**, the NYS **(C)** and the SYS **(D)**.

use a Mo-dependent enzyme, nitrogenase (*Nif*) for N_2 fixation. The study on Mo limitation to N_2 fixation focuses on freshwaters, due to its low dMo concentrations (<20 nmol L^{-1}) and oligotrophic levels. It has been suggested that *Anabaena* had optimal growth at 50-2000 nmol L^{-1} of dMo concentrations (Wolfe, 1954; Tersteeg et al., 1986; Attridge and Rowell, 1997). Mo at 1-5 nmol L^{-1} could limit N_2 fixation (Vasconcelos and Fay, 1974; Zerkle et al., 2006; Glass et al., 2012). However, Mo has long been considered as a potential limiting factor for marine N_2 fixation due to its high seawater value. Several Mo addition experiments in conservative seawaters showed that N_2 fixation rate did not change significantly (Paulsen et al., 1991; Marino et al., 2003). Sulfate inhibition has been considered as an important reason for N_2 fixation role of Mo due to their similar size and stereochemistry (Howarth et al., 1988). In this study, dMo concentrations in seawaters were higher than that in freshwaters, even higher than the Mo limitation in pure cultures, but they were lower than the conservative concentration (~105 nmol L^{-1}). It is unclear about the Mo effect on N_2 fixation in the depleted Mo coastal waters. N_2 fixating and nitrate assimilating cyanobacteria dependent on Mo have been found in the coastal and marine waters, such as *Nostoc* sp. CCMP 2511 (Glass et al., 2010), *Aphanizomenon* sp. (Walve and Larsson, 2007), *Nodularia spumigena* (Walve and Larsson, 2007), *Trichodesmium erythraeum* strain IMS101 (Tuit et al., 2004), *Trichodesmium* (Tuit et al., 2004; Nuester et al., 2012), *Crocosphaera watsonii* strain WH8501 (Tuit et al., 2004). They have Mo:C of 0.2-132, with the highest in *Nostoc* sp. CCMP 2511 (0.2-132) and *Trichodesmium* (9-54). In order to understand the interaction between Mo and N_2 fixation, the NFRs and the relative abundances of cyanobacteria were determined in this study. NFRs and the relative abundances of cyanobacteria presented opposite distributions to Chl-*a*, hinting the competitive growth between phytoplankton and cyanobacteria. The NFRs had a positive correlation with the relative abundance of cyanobacteria (r=0.77, p<0.01; Figure 10A), suggesting that heterocystous cyanobacteria (HC) may be the dominant species of cyanobacteria. The growth of HC likely was more dependent on the availability of Mo than non-HC due to the role of HC in inorganic nitrogen assimilation (Glass et al., 2012). The higher NFRs and relative abundances of cyanobacteria appeared in the SYS with the relatively low nutrient. Particularly, NH_4-N had an opposite distribution to NFRs (r= -0.57, p<0.01; Figure 10B), suggesting that lower NH_4-N was more conducive to N_2 fixation. The depleted dMo concentrations (<90 nmol L^{-1}, except for the BS) negatively correlated with NFRs (r=-0.47, p<0.05; Figure 10C), indicating that the potential effect of Mo on N_2 fixation in the most stations of the YS with the depleted dMo. The relatively conservative dMo in 36 °N section corresponded to higher NFRs and lower Chl-*a*, indicating that phytoplankton uptake is the main removal mechanism of dMo with HC nitrogenase utilization playing a minor role.

Mo is also required for reduction of NO_3^- to NO_2^- through protein nitrate reductase. It has been found that low freshwater Mo concentrations may limit the function of Mo-based nitrogenase and nitrate reductase, thus slowing the growth of cyanobacteria (Glass et al., 2010). In our study, the lower dMo in surface seawaters corresponding to NO_2-N maxima within the BS, and while the dMo maxima corresponding to the lower NO_2-N in 36°N of the YS.

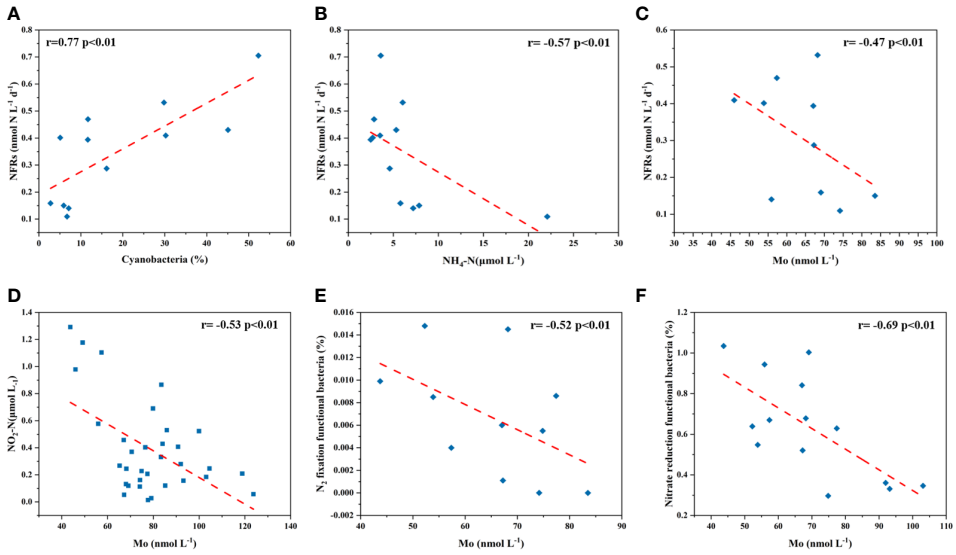

FIGURE 10
Correlations of the relative abundance of cyanobacteria with NFRs **(A)**, NH_4-N with NFRs **(B)** in the BS and YS, dMo (<90 nmol L^{-1}) with NFRs in the YS **(C)**, dMo with NO_2-N **(D)**, dMo with N_2 fixation functional bacteria **(E)** and dMo with nitrate reduction functional bacteria **(F)** in the BS and YS.

NO_2-N concentrations negatively correlated with dMo concentrations (r= -0.53, p<0.01; Figure 10D). These correlations suggested that dMo was involved in nitrate reduction in the study area.

The function prediction of N_2 fixation and nitrate reduction among 16s rRNA data was performed by the FAPROTAX software, which maintains a functional classification database based on species information (Louca et al., 2016). Prediction results showed that the relative abundances of bacteria with N_2 fixation and nitrate reduction genes were small, accounting for 0.001-0.01% and 0.2-1.1% of total bacterial, respectively. The highest N_2 fixation bacteria abundance occurred in south of the SYS (Figure 11), corresponding to the lower dMo and Chl-*a* and higher NFRs. The highest nitrate reduction bacteria abundance occurred in the BS (Figure 11), corresponding to the lower dMo and highest NO_2-N. The dMo concentrations negatively correlated with the relative abundances of bacteria with N_2 fixation (r= -0.52, p<0.01; Figure 10E) and nitrate reduction function (r= -0.69, p<0.01; Figure 10F), suggesting the involving of Mo in N cycling in the BS and SYS. Based on Chl-*a*, nutrients, NFR, function prediction and dMo data, it can be suggested that both the utilization of phytoplankton and nitrate reductase were the main biological pathways of dMo removal in the BS, the utilization of phytoplankton, nitrate reductase and HC nitrogenase were the main biological approaches of dMo removal in the NYS, nitrogenase utilization was the main biological pathway of dMo removal in south of the SYS, whereas dMo in north of the SYS (near 36 °N section) was not affected by biological activity. According to biological abundance, the contribution of biological activities to depleted dMo in the sea area affected by two to three biological activities was in the order of phytoplankton uptake, nitrate reductase and nitrogenase utilization. It has been shown that N_2 fixation required more Mo than NO_3-N assimilation in freshwater (Attridge and Rowell, 1997; Glass et al., 2010; Glass et al., 2012). The contrary phenomenon was found in our study. It seems that although depleted dMo in the BS and YS, its concentration was still higher than freshwater, resulting in the less limitation on N_2 fixation.

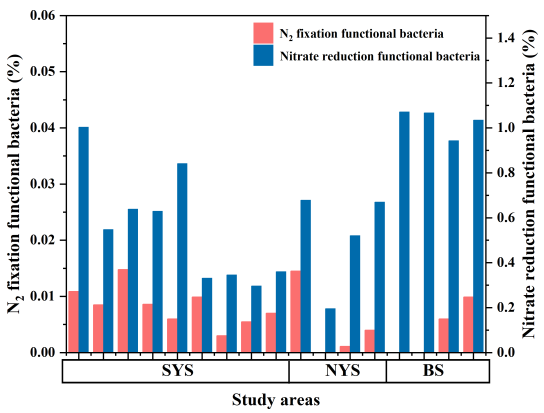

FIGURE 11
The relative abundances of bacteria with N_2 fixation and nitrate reduction function. The function prediction was performed by the FAPROTAX software based on 16s rRNA data.

5 Conclusions

Molybdenum behavior and it involving into nitrogen cycling in the BS and YS were studied. DMo concentrations in the BS and YS (except for 36 °N section) were significantly below those expected for a conservative mixing, indicating nonconservative behavior of dMo. The removal pathways of dMo in the BS and YS included scavenging by Mn-oxides, upward transport block due to water stratification and sediment Mo enrichment in low DO level of the YSCW, phytoplankton uptake and involving in N cycling. Based on the hydrochemical and biological data, it can be concluded that the combined effect of inorganic particle adsorption and biological utilization, especially phytoplankton and nitrate reductase utilization, was the removal mechanism of dMo in the BS and NYS. Biological uptake, especially nitrogenase utilization, was the main removal pathway of dMo in south of the SYS. These removal mechanisms induced the depleted dMo in the BS and YS (except for north of the SYS near 36°N section). The relatively conservative Mo in the 36°N section corresponding to the higher dMn and NFRs, and the lower Chl-*a* and NO_2-N, suggesting it involving in N_2 fixation. However, the nitrogenase utilization of dMo was small due to low cyanobacteria abundance.

Data availability statement

The datasets presented in this study are available in the NCBI SRA repositories. The names of the repository/repositories and accession number(s) can be found below: SRR22378289–SRR22378306.

Author contributions

JF, methodology, conceptualization, formal analysis, investigation, and writing original draft. LD, methodology, conceptualization, resources, writing original draft, review and editing, and supervision. MY, formal analysis, and investigation. HY and XL, formal analysis. All authors contributed to the article and approved the submitted version.

Funding

This work was supported by the National Natural Science Foundation of China (No. 41976037), Shandong Provincial

Natural Science Foundation (ZR2020YQ28), the Taishan Scholars Program, Wenhai Program of QNLM (NO. 2021WHZZB0903), Yantai "Double Hundred Plan" funding project, and National Natural Science Foundation of China (No. 41906035). Samples were collected onboard of R/V *Lan Hai 101* implementing the open research cruise NORC2021-01 supported by NSFC Shiptime Sharing Project (No. 42049901).

Conflict of interest

The authors declare that the research was conducted in the absence of any commercial or financial relationships that could be construed as a potential conflict of interest.

Publisher's note

Supplementary material

The Supplementary Material for this article can be found online at: https://www.frontiersin.org/articles/10.3389/fmars.2022.1094846/full#supplementary-material

References

Archer, C., and Vance, D. (2008). The isotopic signature of the global riverine molybdenum flux and anoxia in the ancient oceans. *Nat. Geosci.* 1, 597–600. doi: 10.1038/ngeo282

Attridge, E. M., and Rowell, P. (1997). Growth, heterocyst differentiation and nitrogenase activity in the cyanobacteria *Anabaena variabilis* and *Anabaena cylindrica* in response to molybdenum and vanadium. *New Phytol.* 135, 517–526. doi: 10.1046/j.1469-8137.1997.00666.x

Audry, S., Blanc, G., Schafer, J., Guerin, F., Masson, M., and Robert, S. (2007). Budgets of Mn, cd and Cu in the macrotidal gironde estuary (SW France). *Mar. Chem.* 107, 433–448. doi: 10.1016/j.marchem.2007.09.008

Barton, L. L., Goulhen, F., Bruschi, M., Woodards, N. A., Plunkett, R. M., and Rietmeijer, F. J. M. (2007). The bacterial metallome: Composition and stability with specific reference to the anaerobic bacterium *Desulfovibrio desulfuricans*. *Biometals* 20, 291–302. doi: 10.1007/s10534-006-9059-2

Beck, M., Dellwig, O., Fischer, S., Schnetger, B., and Brumsack, H. J. (2012). Trace metal geochemistry of organic carbon-rich watercourses draining the NW German coast. *Estuar. Coast. Shelf Sci.* 104, 66–79. doi: 10.1016/j.ecss.2012.03.025

Brumsack, H. J. (2006). The trace metal content of recent organic carbon-rich sediments: Implications for Cretaceous black shale formation. *Palaeogeogr. Palaeoclimatol. Palaeoecol.* 232, 344–336. doi: 10.1016/j.palaeo.2005.05.011

Bryan, J. R., Riley, J. P., and Williams, P. J. L. (1976). Winkler procedure for making precise measurements of oxygen concentration for productivity and related studies. *J. Exp. Mar. Biol. Ecol.* 21, 191–197. doi: 10.1016/0022-0981(76)90114-3

Chen, C. T. A. (2009). Chemical and physical fronts in the bohai, yellow and East China seas. *J. Mar. Syst.* 78, 394–410. doi: 10.1016/j.jmarsys.2008.11.016

Chen, J. B., Gaillardet, J., Bouchez, J., Louvat, P., and Wang, Y. N. (2014). Anthropophile elements in river sediments: Overview from the seine river, France. *Geochem. Geophys. Geosyst.* 15, 4526–4546. doi: 10.1002/2014gc005516

Collier, R. W. (1985). Molybdenum in the northeast pacific ocean. *Limnol. Oceanogr.* 30, 1351–1354. doi: 10.4319/lo.1985.30.6.1351

Dalai, T. K., Nishimura, K., and Nozaki, Y. (2005). Geochemistry of molybdenum in the chao phraya river estuary, Thailand: Role of suboxic diagenesis and porewater transport. *Chem. Geol.* 218, 189–202. doi: 10.1016/j.chemgeo.2005.01.002

Dellwig, O., Beck, M., Lemke, A., Lunau, M., Kolditz, K., Schnetger, B., et al. (2007). Non-conservative behaviour of molybdenum in coastal waters: Coupling geochemical, biological, and sedimentological processes. *Geochim. Cosmochim. Acta*71, 2745–2761. doi: 10.1016/j.gca.2007.03.014

Fay, P., and Fogg, G. E. (1962). Studies on nitrogen fixation by blue-green algae III. growth and nitrogen fixation in chlorogloea fritschii mitra. *Arch. Mikrobiol.* 42, 310–321. doi: 10.1007/bf00422048

Firdaus, M. L., Norisuye, K., Nakagawa, Y., Nakatsuka, S., and Sohrin, Y. (2008). Dissolved and labile particulate zr, hf, Nb, Ta, Mo and W in the western north pacific ocean. *J. Oceanogr.* 64, 247–257. doi: 10.1007/s10872-008-0019-z

Fischer, K., Barbier, G. G., Hecht, H. J., Mendel, R. R., Campbell, W. H., and Schwarz, G. (2005). Structural basis of eukaryotic nitrate reduction: Crystal structures of the nitrate reductase active site. *Plant Cell* 17, 1167–1179. doi: 10.1105/tpc.104.029694

Fowler, D., Pyle, J. A., Raven, J. A., and Sutton, M. A. (2013). The global nitrogen cycle in the twenty-first century: Introduction. *Philos. Trans. R. Soc B Biol. Sci.* 368, 20130165. doi: 10.1098/rstb.2013.0165

Glass, J. B., Axler, R. P., Chandra, S., and Goldman, C. R. (2012). Molybdenum limitation of microbial nitrogen assimilation in aquatic ecosystems and pure cultures. *Front. Microbiol.* 3, 1–11. doi: 10.3389/fmicb.2012.00331

Glass, J. B., Wolfe-Simon, F., Elser, J. J., and Anbar, A. D. (2010). Molybdenum-nitrogen co-limitation in freshwater and coastal heterocystous cyanobacteria. *L* 55, 667–676. doi: 10.4319/lo.2009.55.2.0667

Goldman, C. R. (1960). Molybdenum as a factor limiting primary productivity in castle lake, California. *Science* 132, 1016–1017. doi: 10.1126/science.132.3433.1016

Guo, S. J., Li, Y. Q., Zhang, C. X., Zhai, W. D., Huang, T., Wang, L. F., et al. (2014). Phytoplankton community in the bohai Sea and its relationship with environmental factors. *Mar. Sci. Bull.* 33, 95–105 doi: 10.11840/j.issn.1001-6392.2014.01.013

Guo, J. Q., Yuan, H. M., Song, J. M., Li, X. G., and Duan, L. Q. (2020). Hypoxia, acidification and nutrient accumulation in the yellow Sea cold water of the south yellow Sea. *Sci. Total Environ.* 745, 141050. doi: 10.1016/j.scitotenv.2020.141050

Head, P. C., and Burton, J. D. (1970). Molybdenum in some ocean and estuarine waters. *J. Mar. Biol. Assoc. U. K.* 50, 439–448. doi: 10.1017/s002531540000463x

Ho, P., Lee, J. M., Heller, M. I., Lam, P. J., and Shiller, A. M. (2018). The distribution of dissolved and particulate Mo and V along the US GEOTRACES East pacific zonal transect (GP16): The roles of oxides and biogenic particles in their distributions in the oxygen deficient zone and the hydrothermal plume. *Mar. Chem.* 201, 242–255. doi: 10.1016/j.marchem.2017.12.003

Ho, T. Y., Quigg, A., Finkel, Z. V., Milligan, A. J., Wyman, K., Falkowski, P. G., et al. (2003). The elemental composition of some marine phytoplankton. *J. Phycol.* 39, 1145–1159. doi: 10.1111/j.0022-3646.2003.03-090.x

Howarth, R. W., and Cole, J. J. (1985). Molybdenum availability, nitrogen limitation, and phytoplankton growth in natural waters. *Science* 229, 653–655. doi: 10.1126/science.229.4714.653

Howarth, R. W., Marino, R., Lane, J., and Cole, J. J. (1988). Nitrogen-fixation in fresh-water, estuarine, and marine ecosystems I.rates and importance. *Limnol. Oceanogr.* 33, 669–687. doi: 10.4319/lo.1988.33.4_part_2.0669

Khan, S. H., and Van Den Berg, C. M. G. (1989). The determination of molybdenum in estuarine waters using cathodic stripping voltammetry. *Mar. Chem.* 27, 31–42. doi: 10.1016/0304-4203(89)90026-1

Kowalski, N., Dellwig, O., Beck, M., Grunwald, M., Fischer, S., Piepho, M., et al. (2009). Trace metal dynamics in the water column and pore waters in a temperate tidal system: Response to the fate of algae-derived organic matter. *Ocean Dynami.* 59, 333–350. doi: 10.1007/s10236-009-0192-7

Linnik, P. N., Zhezherya, V. A., Linnik, R. P., Ignatenko, I. I., and Zubenko, I. B. (2015). Metals in surface water of Ukraine: The migration forms, features of distribution between the abiotic components of aquatic ecosystems, and potential bioavailability. *Russ. J. Gen. Chem.* 85, 2965–2984. doi: 10.1134/s1070363215130162

Liu, S. M., Li, L. W., and Zhang, Z. N. (2011). Inventory of nutrients in the bohai. *Continent. Shelf Res.* 31, 1790–1797. doi: 10.1016/j.csr.2011.08.004

Louca, S., Parfrey, L. W., and Doebeli, M. (2016). Decoupling function and taxonomy in the global ocean microbiome. *Science* 353, 1272–1277. doi: 10.1126/science.aaf4507

Marino, R., Howarth, R. W., Chan, F., Cole, J. J., and Likens, G. E. (2003). Sulfate inhibition of molybdenum-dependent nitrogen fixation by planktonic cyanobacteria under seawater conditions: A non-reversible effect. *Hydrobiologia* 500, 277–293. doi: 10.1023/a:1024641904568

Mendel, R. R. (2009). Cell biology of molybdenum. *Biofactors* 35, 429–434. doi: 10.1002/biof.55

Mohajerin, T. J., Helz, G. R., and Johannesson, K. H. (2016). Tungsten-molybdenum fractionation in estuarine environments. *Geochim. Cosmochim. Acta* 177, 105–119. doi: 10.1016/j.gca.2015.12.030

Mohr, W., Grosskopf, T., Wallace, D. W. R., and LaRoche, J. (2010). Methodological underestimation of oceanic nitrogen fixation rates. *PloS One* 5, 7. doi: 10.1371/journal.pone.0012583

Morford, J. L., and Emerson, S. (1999). The geochemistry of redox sensitive trace metals in sediments. *Geochim. Cosmochim. Acta* 63, 1735–1750. doi: 10.1016/s0016-7037(99)00126-x

Morford, J. L., Martin, W. R., Kalnejais, L. H., Francois, R., Bothner, M., Karle, I. M., et al. (2007). Insights on geochemical cycling of U, re and Mo from seasonal sampling in Boston harbor. *Geochim. Cosmochim. Acta* 71, 895–917. doi: 10.1016/j.gca.2006.10.016

Nagler, T.F., Neubert, N., Bottcher, M. E., Dellwig, O., and Schnetger, B. (2011). Molybdenum isotope fractionation in pelagic euxinia: Evidence from the modern Black and Baltic Seas. *Chem. Geol.* 289, 1–11. doi: 10.1016/j.chemgeo.2011.07.001

Nakagawa, Y., Takano, S., Firdaus, M. L., Norisuye, K., Hirata, T., Vance, D., et al. (2012). The molybdenum isotopic composition of the modern ocean. *Geochem. J.* 46, 131–141. doi: 10.2343/geochemj.1.0158

Neal, C., and Robson, A. J. (2000). A summary of river water quality data collected within the land-ocean interaction study: Core data for eastern UK rivers draining to the north Sea. *Sci. Total Environ.* 251, 585–665. doi: 10.1016/s0048-9697(00)00397-1

Nuester, J., Vogt, S., Newville, M., Kustka, A. B., and Twining, B. S. (2012). The unique biogeochemical signature of the marine diazotroph *Trichodesmium*. *Front. Microbiol.* 3. doi: 10.3389/fmicb.2012.00150

Paulsen, D. M., Paerl, H. W., and Bishop, P. E. (1991). Evidence that molybdenum-dependent nitrogen fixation is not limited by high sulfate concentrations in marine environments. *Limnol. Oceanogr.* 36, 1325–1334. doi: 10.4319/lo.1991.36.7.1325

Prange, A., and Kremling, K. (1985). Distribution of dissolved molybdenum, uranium and vanadium in baltic sea waters. *Mar. Chem.* 16, 259–274. doi: 10.1016/0304-4203(85)90066-0

Qu, P. P., Fu, F. X., Wang, X. W., Kling, J. D., Elghazzawy, M., Huh, M., et al. (2022). Two co-dominant nitrogen-fixing cyanobacteria demonstrate distinct acclimation and adaptation responses to cope with ocean warming. *Environ. Microbiol. Rep.* 14, 203–217. doi: 10.1111/1758-2229.13041

Rahaman, W., Singh, S. K., and Raghav, S. (2010). Dissolved Mo and U in rivers and estuaries of India: Implication to geochemistry of redox sensitive elements and their marine budgets. *Chem. Geol.* 278, 160–172. doi: 10.1016/j.chemgeo.2010.09.009

Reitz, A., Wille, M., Nagler, T. F., and de Lange, G. J. (2007). Atypical Mo isotope signatures in eastern Mediterranean sediments. *Chem. Geolo.* 245, 1–8. doi: 10.1016/j.chemgeo.2007.06.018

Robson, R. L., Eady, R. R., Richardson, T. H., Miller, R. W., Hawkins, M., and Postgate, J. R. (1986). The alternative nitrogenase of *Azotobacter chroococcum* is a vanadium enzyme. *Nature* 322, 388–390. doi: 10.1038/322388a0

Schneider, A. B., Koschinsky, A., Kiprotich, J., Poehle, S., and do Nascimento, P. C. (2016). An experimental study on the mixing behavior of Ti, zr, V and Mo in the Elbe, Rhine and weser estuaries. *Estuar. Coast. Shelf Sci.* 170, 34–44. doi: 10.1016/j.ecss.2015.12.002

Scott, C., Lyons, T. W., Bekker, A., Shen, Y., Poulton, S. W., Chu, X., et al. (2008). Tracing the stepwise oxygenation of the proterozoic ocean. *Nature* 452, 456–459. doi: 10.1038/nature06811

Smedley, P. L., and Kinniburgh, D. G. (2017). Molybdenum in natural waters: A review of occurence, distributions and controls. *Appl. Geochem.* 84, 387–432. doi: 10.1016/j.apgeochem.2017.05.008

Stiefel, E. I. (1996). Molybdenum bolsters the bioinorganic brigade. *Science* 272, 1599–1600. doi: 10.1126/science.272.5268.1599

Strady, E., Blanc, G., Schafer, J., Coynel, A., and Dabrin, A. (2009). Dissolved uranium, vanadium and molybdenum behaviours during contrasting freshwater discharges in the gironde estuary (SW France). *Estuar. Coast. Shelf Sci.* 8, 550–560. doi: 10.1016/j.ecss.2009.05.006

Sulu-Gambari, F., Roepert, A., Jilbert, T., Hagens, M., Meysman, F. J. R., and Slomp, C. P. (2017). Molybdenum dynamics in sediments of a seasonally-hypoxic coastal marine basin. *Chem. Geol.* 466, 627–640. doi: 10.1016/j.chemgeo.2017.07.015

Tersteeg, P. F., Hanson, P. J., and Paerl, H. W. (1986). Growth-limiting quantities and accumulation of molybdenum in *Anabaena oscillarioides* (Cyanobacteria). *Hydrobiologia* 140, 143–147. doi: 10.1007/bf00007567

Tuit, C. B., and Ravizza, G. (2003). The marine distribution of molybdenum. *Geochim. Cosmochim. Acta* 67, A495–A495.

Tuit, C., Waterbury, J., and Ravizza, G. (2004). Diel variation of molybdenum and iron in marine diazotrophic cyanobacteria. *Limnol. Oceanogr.* 49, 978–990. doi: 10.4319/lo.2004.49.4.0978

Valdivieso-Ojeda, J. A., Huerta-Diaz, M. A., and Delgadillo-Hinojosa, F. (2020). Non-conservative behavior of dissolved molybdenum in hypersaline waters of the Guerrero Negro saltern, Mexico. *Appl. Geochem.* 115, 104565. doi: 10.1016/j.apgeochem.2020.104565

Vasconcelos, L. D., and Fay, P. (1974). Nitrogen metabolism and ultrastructure in *Anabaena cylindrica* I. the effect of nitrogen starvation. *Arch. Microbiol.* 96, 271–279. doi: 10.1007/bf00590183

Waeles, M., Dulaquais, G., Jolivet, A., Thebault, J., and Riso, R. D. (2013). Systematic non-conservative behavior of molybdenum in a macrotidal estuarine system (Aulne-bay of Brest, France). *Estuar. Coast. Shelf Sci.* 131, 310–318. doi: 10.1016/j.ecss.2013.06.018

Walve, J., and Larsson, U. (2007). Blooms of Baltic Sea *Aphanizomenon* sp. (Cyanobacteria) collapse after internal phosphorus depletion. *Aquat. Microb. Ecol. Proc. Conf.* 49, 57–69. doi: 10.3354/ame01130

Wang, B., Hirose, N., Kang, B., and Takayama, K. (2014). Seasonal migration of the yellow Sea bottom cold water. *J. Geophys. Res-Oceans* 119, 4430–4443. doi: 10.1002/2014jc009873

Wang, D. L., Xia, W. W., Lu, S. M., Wang, G. Z., Liu, Q., Moore, W. S., et al. (2016). The nonconservative property of dissolved molybdenum in the western Taiwan strait: Relevance of submarine groundwater discharges and biological utilization. *Geochem. Geophys. Geosyst.* 17, 28–43. doi: 10.1002/2014gc005708

Wolfe, M. (1954). The effect of molybdenum upon the nitrogen metabolism of *Anabaena cylindrica* I. a study of the molybdenum requirement for nitrogen fixation and for nitrate and ammonia assimilation. *Ann. Bot.* 18, 299–308. doi: 10.1093/oxfordjournals.aob.a083396

Xin, M., Wang, B. D., Xie, L. P., Sun, X., Wei, Q. S., Mang, S. K., et al. (2019). Long-term changes in nutrient regimes and their ecological effects in the bohai Sea, China. *Mar. pollut. Bull.* 146, 562–573. doi: 10.1016/j.marpolbul.2019.07.011

Xu, B. C., Burnett, W., Dimova, N., Diao, S. B., Mi, T. Z., Jiang, X. Y., et al. (2013). Hydrodynamics in the yellow river estuary via radium isotopes: Ecological perspectives. *Cont. Shelf Res.* 66, 19–28. doi: 10.1016/j.csr.2013.06.018

Zehr, J. P., and Capone, D. G. (2020). Changing perspectives in marine nitrogen fixation. *Science* 368, eaay9514. doi: 10.1126/science.aay9514

Zerkle, A. L., House, C. H., Cox, R. P., and Canfield, D. E. (2006). Metal limitation of cyanobacterial N_2 fixation and implications for the precambrian nitrogen cycle. *Geobiology* 4, 285–297. doi: 10.1111/j.1472-4669.2006.00082.x

Zerkle, A. L., Scheiderich, K., Maresca, J. A., Liermann, L. J., and Brantley, S. L. (2011). Molybdenum isotope fractionation by cyanobacterial assimilation during nitrate utilization and N_2 fixation. *Geobiology* 9, 94–106. doi: 10.1111/j.1472-4669.2010.00262.x

Zhai, W. D. (2018). Exploring seasonal acidification in the yellow Sea. *Sci. China-Earth Sci.* 61, 647–658. doi: 10.1007/s11430-017-9151-4

Zhang, Z. X., Qiao, F. L., Guo, J. S., and Guo, B. H. (2018). Seasonal changes and driving forces of inflow and outflow through the bohai strait. *Cont. Shelf Res.* 154, 1–8. doi: 10.1016/j.csr.2017.12.012

Zheng, L. W., and Zhai, W. D. (2021). Excess nitrogen in the bohai and yellow seas, China: Distribution, trends, and source apportionment. *Sci. Total Environ.* 794, 148702. doi: 10.1016/j.scitotenv.2021.148702